IMPERIAL
Grantham Institute

Institute reports and analytical notes

Summer heat deaths in 854 European cities more than tripled due to climate change

2025

Contents

Key points

- Extreme heat is the deadliest type of weather and officially reported heat deaths remain significantly underestimated. We use established peer-reviewed methodology to estimate the total number of heat-related deaths in 854 cities during the recent heatwave and to calculate the proportion of these deaths that can be attributed to climate change. In total, we estimate climate change driven changes to the temperatures to have caused 16,469 additional excess deaths (95% empirical Confidence Intervals: 15,013 to 17,864) across the 854 cities, accounting for almost 70% of the estimated summer deaths.
- June-August 2025 was the fourth warmest summer season on record, 0.9°C above the 1990-2020 mean. This means a seriously heightened risk of death for vulnerable people, including those over 65 and with preexisting medical conditions, as well as increased risk of overheating of indoor environments. All of this comes with an increasing high demand for health services and increased power demand.
- We use both observations-based products and climate models to estimate that summer temperatures across Europe are now 1.5 to 2.9°C than they would have been in a 1.3°C cooler climate, without human-caused climate change caused primarily by the burning of fossil fuels. However, this is probably a conservative estimate of the true warming experienced in many cities, as climate models are known to underestimate warming in Europe.
- Among 30 European capitals, Rome, Athens, and Bucharest had the highest estimated excess mortality per population this summer. The largest relative proportions of heat-related deaths were observed in Stockholm, Madrid, and Bratislava, with more than 85% of the estimated summer deaths to be attributed to climate change.
- The study did not investigate the factors that influenced the deaths estimated in each city or the current level of preparedness for mitigating the heat-related health risks. It is likely that most deaths estimated here reflect the intensity of heat experienced by each city this summer, but factors including population demographics, air pollution and adaptation to heat are also known to play an important role.
- The study looks at 854 cities in the EU and affiliated countries. This covers only about 30% of the population of Europe and so cannot be taken as indicative of the total number of excess deaths. A range of limitations may have influenced the estimates, including climate models that are known to underestimate the rate of warming, an event definition that does not capture the most intense peaks in daily temperatures and exposure-response functions that do not consider attenuation to heat in recent years.
- Cities are highly vulnerable to heatwaves because large amounts of concrete and asphalt surfaces trap and hold heat, while transport and energy use generate even more, intensifying dangerous urban temperatures. Expanding green and blue spaces are known to decrease this urban heat island effect and provide crucial cooler spaces that can be lifelines for people in heatwaves, particularly lower socioeconomic groups that live in denser housing and are less likely to have air conditioning. Urbanisation is an increasing trend in Europe with 70% of people living in cities and more than 80% expected by 2050. The converging trends

of urbanisation, ageing population and climate change drive vulnerability and increase the risk of reaching limits to adaptation.

- Current policies in place around the world are projected to result in about 2.7°C of warming above pre-industrial levels by 2100, which would result in many more heat-related deaths and impacts globally. This highlights yet again the urgent need to rapidly transition away from fossil fuels to secure a liveable future.

Introduction

Summer 2025 has been "roasting hot" across Europe, with back-to-back heatwaves affecting both humans and the economy (Guglielmi, 2025). Peaking in mid-June to early July across different regions, Western Europe as a whole experienced its highest average temperatures for this period in decades, and the hottest June on record (ibid.). Temperatures rose above 40°C, and up to 46°C in Spain and Portugal, due to a persistent high-pressure system, also known as a heat dome, causing it to stay hotter for longer (ibid.). Fennoscandia also experienced an exceptionally persistent heatwave in July, including the longest streak of daily maximum temperatures reaching 25°C ever observed in Finnish Lapland - 26 consecutive days (Barnes et al., 2025). Southeast Europe faced heatwaves in July and a national record temperature of 50.5°C was recorded in Türkiye (Copernicus, 2025).

In August, the entire Mediterranean region of Europe, especially the Iberian Peninsula, was affected by another intense heat wave, reinforced by both a heat dome and a heat plume, the rising of hot air masses from North Africa and the Iberian Peninsula (Le Monde, 2025). Spain recorded its most intense heat wave ever, exceeding the 2022 event with a temperature anomaly of 4.6°C, according to provisional data from Spanish State Meteorological Agency AEMET (Euronews, 2025). From 8 to 17 August, Spain experienced the hottest ten-day period ever recorded since 1950 at least (Euronews, 2025). Unprecedented heat levels were also recorded from the southwest to the center-east of France, as well as near the Mediterranean (Météo France, 2025).

At the European scale, June 2025 was the fifth-warmest June on record (Copernicus, 2025a), while July 2025 ranked as the fourth-warmest July on record (Copernicus, 2025b), and August the third warmest August (Copernicus, 2025c). Overall, it was the fourth warmest summer season on record, 0.9°C above the 1990-2020 mean (ibid.). When looking at the summer of 2025 as a whole and individual countries, it was the warmest on record for the UK, with a mean temperature of 16.10°C, surpassing the previous record of 15.76°C set in 2018 (Met Office, 2025). France had its third hottest summer on record, behind the summers of 2003 and 2022 (Météo France, 2025). However, parts of eastern Europe, including the Baltic states, Belarus and Poland, were slightly cooler than the 1990-2020 average (Figure 1).

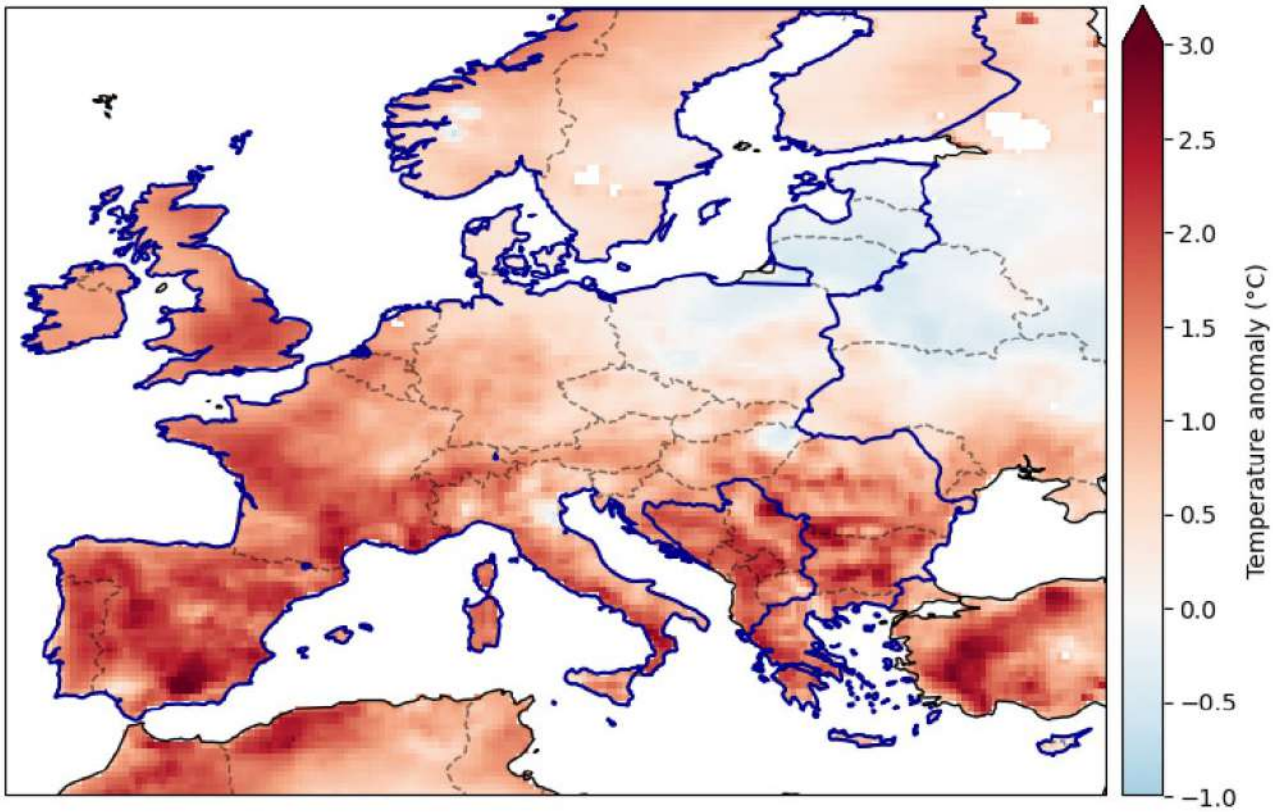

Figure 1: *Mean temperature anomaly in June-August 2025 compared to 1990-2020 climatology (ERA5). The dark blue line indicates the regions considered within this study, which is bounded by the domain 11W, 35E; 33N, 66N.*

While the temperatures reached across the continent in 2025 were unusually warm, temperatures across Europe are known to be increasing more rapidly than the rest of the world (Copernicus, 2024), and there is an extensive body of literature attributing this with high confidence to human influence on the climate (Seneviratne et al., 2021; Quilcaille et el., 2025).

Heat, extreme heat and heatwaves affect human health and well-being. The European Environment Agency (EEA) describes heat as “the largest and most urgent climate hazard for human health” (EEA, 2024). In the past, Europe has recorded thousands of excess heat-related deaths each year (Masselot, et. al., 2023, Ballester et al., 2023). During the summer of 2022, more than 60,000 people across Europe died as a result of extreme heat (Ballester et al., 2023). An impact attribution study found that 56% of these excess deaths could be attributed to human-induced climate change (Beck et al., 2024). Even in the following summer, which was less intensely hot, over 47,000 heat-related deaths were recorded (Gallo et al., 2024). A global study recently showed that 178,000 deaths can be linked to heatwaves in 2023 and that more than half (54.29%) of these deaths are attributable to climate change (Hundessa et al., 2025). It also found that the highest mortality rates and excess death ratios occurred in Southern, Eastern and Western Europe, amounting to a total of 66,443 for the continent (Hundessa et al., 2025).

Among other factors, population age structure and socio-economic drivers determine vulnerability to high temperatures (Falchetta et al., 2024). Europe's population is projected to age significantly

(Eurostat, 2023), and by 2050, a substantial share of Europe's population is expected to be exposed to extreme heat (Falchetta et al., 2024). Under a 2°C global warming scenario, approximately 163 million Europeans could face unprecedented summer temperatures, nearly twice the number currently affected (King et, al., 2018; Garcia-Leon et al., 2024). While there is quantitative evidence that adaptation to extreme heat is taking place to a certain extent in some places (Vicedo-Cabrera et al., 2018, Stuart-Smith et al., 2025), large adaptation gaps still prevail and future impacts from extreme heat can still be avoided.

Beyond causing deaths, heat increases hospitalisations and worsens chronic illnesses, especially for older adults and low-income communities (World Bank, 2025). Livelihoods and economic activities are threatened as jobs in informal services, construction, transport and tourism are particularly hit (World Bank, 2025).

Adaptation to heat

Cities are hotspots of heat risk due to the urban heat island effect, rapidly ageing populations, and urban growth pressures; urbanisation is an increasing trend in Europe with 70% of people living in cities and more than 80% expected by 2050 (World Bank, 2025; European Commission, 2025a). A wide portfolio of adaptation measures is required to reduce impacts: from early-warning systems and timely advice to the public to the enhancement of housing and urban planning (such as expanding green spaces), reinforced healthcare and social services and the adjustment of working conditions and activities during periods of extreme heat (EEA, 2025). While impacts of heat on human health are recognised in a large share of national adaptation and health policies and strategies, the level of policy preparedness to heat for Europe is assessed as 'medium' by the European Climate Risk Assessment, due to aspects of social justice often missing in planning instruments (EEA, 2024). Heat-health action plans are a key tool to reduce deaths during extreme heat, as they aim to assign responsibilities in the event of an emergency and plan both short- and long-term measures to reduce risks (EEA, 2025). Current mitigation policies in place around the world are projected to result in about 2.7°C warming above pre-industrial levels by 2100 (Climate Action Tracker, 2024), which would result in many more heat-related deaths and impacts globally. Research has shown that both stringent mitigation and adaptation must be implemented in parallel, as it is becoming increasingly challenging to adapt (Masselot, 2025) and limits to adaptation are being reached (IPCC, 2022).

In addition, as the results presented here and large literature on vulnerability to heat shows, older people are particularly vulnerable. Even if the frequency or intensity of climate hazards were to remain constant due to effective mitigation, collective risks from extreme weather events have the potential to increase significantly in the future due to an ageing population (Harrington and Otto, 2023; European Commission, 2025b). While policies promoting sustainable development inherently support communities in managing the risks associated with extreme weather over the coming decades, additional targeted strategies will be necessary to address the unique challenges posed by rapidly growing older populations projected under different development pathways. Failing to account for these demographic risks could further complicate efforts to achieve well-being and resilience in a warming climate.

Study aims & scope

This study first uses an established extreme event attribution methodology to analyse changes in monthly mean temperatures during the summer months of 2025 in 854 cities across Europe (Figure 2), and the extent to which those changes can be attributed to human-caused warming. We use this attributable change in intensity to estimate how much cooler the daily mean temperatures would have been throughout the summer months, if human activities had not warmed the planet by 1.3°C above preindustrial levels. We use established exposure-response relationships (Masselot et al., 2023) to estimate the excess mortality attributed to heat given the observed temperatures and also under the counterfactual scenario of a 1.3°C cooler world. By comparing these estimates, we calculate how many more people are expected to have died in each city during the summer of 2025 due to the excess heat caused by anthropogenic warming. We also report the expected proportion of heat-related deaths attributed to human-induced climate change. The 854 cities represent all cities in the EU and affiliated countries (including Switzerland and the UK) with more than 50,000 inhabitants, totalling an estimated 30% of the total population of Europe.

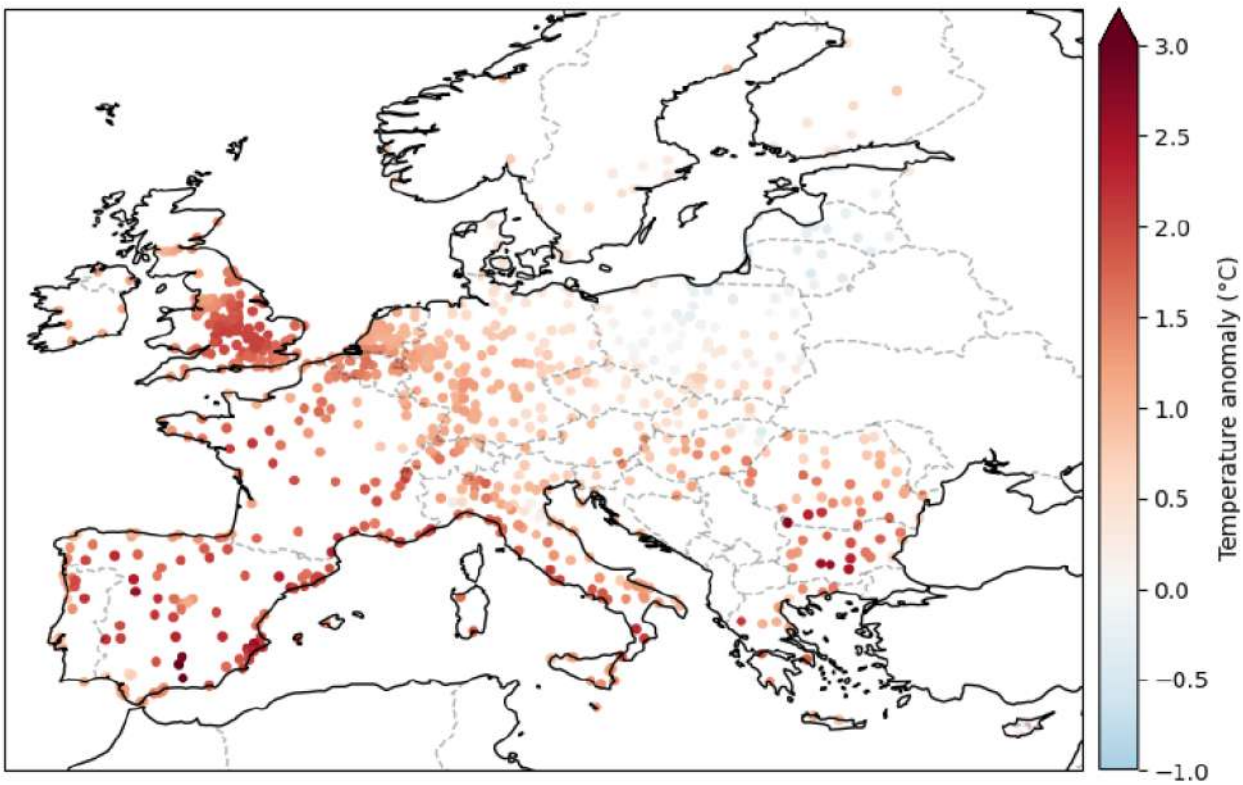

***Figure 2**: Mean temperature anomaly June-August 2025 compared to 1990-2020 climatology in each of the 854 cities included in the study (ERA5).*

At the time of writing, the actual number of deaths reported during the study period was not yet available; therefore, the numbers reported here should be interpreted as estimates of expected heat related mortality rather than actual outcomes. Briefly, to estimate the expected mortality, we use all available historical mortality data for each city to calculate a baseline mortality rate. This rate is assumed to remain constant throughout the year and is projected to apply to the year 2025.

1 Trends in summer temperatures over Europe

1.1 Summer 2025

Summer temperatures in 2025 were around 0.9°C above the 1990-2020 mean over the whole of Europe (Copernicus, 2025c), although there was substantial variability within the region, with southern and eastern Europe experiencing much higher temperatures than northern and western Europe (Figure 3a). With the exception of Estonia, Latvia and Lithuania, all countries within the study region experienced a warmer than average summer (Figure 3b), with much of western and southern Europe experiencing temperatures more than 1°C warmer than the 1990-2020 mean.

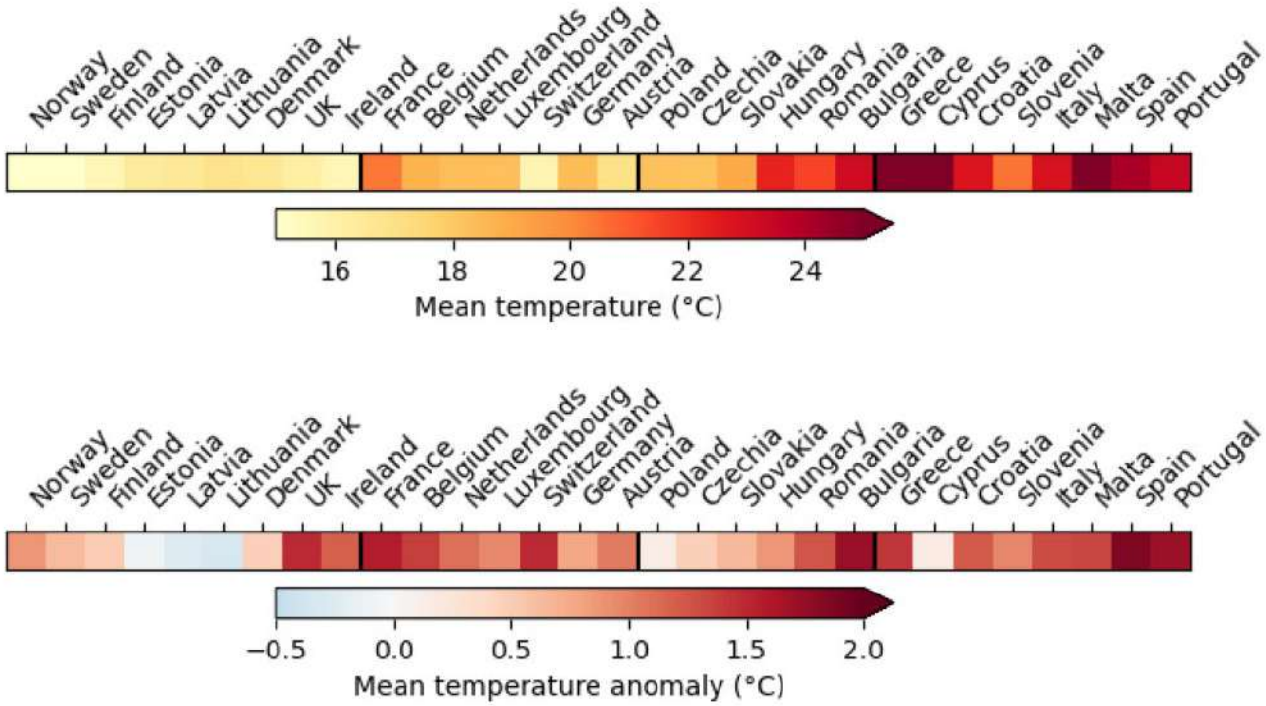

***Figure 3**: (a) mean summer temperatures and (b) mean summer temperature anomaly with respect to 1990-2020 climatology, for all countries within the scope of the study. Mean temperatures are averages over daily mean temperatures from ERA5 reanalysis, encompassing all land grid cells within the domain 11W, 35E; 33N, 66N (shown in Figure 1). Black lines divide countries into Northern, Western, Eastern and Southern regions.*

Figure 4 shows the daily mean temperature anomalies in each country from June-August 2025 with respect to the 1990-2020 daily climatology, highlighting the different spatial patterns of warm periods across the continent. Much of continental Europe was unusually warm throughout June, culminating in a heatwave at the end of the month during which much of western and southern Europe was more than two degrees warmer than usual for the time of year (Figure 4, box 1). Heat health warnings were issued in many cities and the hot, dry conditions led to a reported 300 hospitalisations due to the heat, with eight fatalities reported while the event was still ongoing (ERCC, 2025), as well as creating extremely fire-prone conditions (Clarke et al., 2025).

While much of Europe was slightly cooler throughout July, Scandinavia and the Baltic countries experienced a lengthy heatwave from mid to late July during which multiple heat records were set across Fennoscandia (Figure 4, box 2). Increased heat-related hospitalisations were reported across the region, and numerous wildfires broke out, with the resulting smoke impacting air quality (Barnes et al., 2025). It is important to note that the gridded data used to estimate the national mean temperatures was clipped at 66N in order to ensure that the temperatures reported are more or less representative of those experienced in the cities for which mortality data was available. Moreover, since the highest temperatures and temperature anomalies recorded during this heatwave occurred further north than this, the figures reported here should not be taken as representative of the temperatures over these countries as a whole, which are likely somewhat higher.

A record-breaking week-long heatwave in late July (Figure 4, box 3) in southeast Europe was linked to devastating wildfires in Greece, Cyprus, Türkiye and the rest of the Balkans (Keeping et al., 2025a; EFFIS, 2025). We note that the six Balkan countries outside of the EU are not represented in this study; however, as Figure 1 shows, they also experienced a very warm summer, with the average summer temperature across Albania, Bosnia and Herzegovina, Kosovo, Montenegro, North Macedonia and Serbia more than 1.7°C warmer than the 1990-2020 mean.

In mid-August, a second pan-European heatwave again brought temperatures more than 2°C above the seasonal mean for nearly a week (Figure 4, box 4). In Spain and Portugal, where the heat persisted for several weeks, this was one of the most intense heatwaves on record, again coinciding with record-breaking levels of wildfire activity (Keeping et al., 2025b).

For the four periods of extreme heat highlighted in Figure 4 (dark blue boxes), unusually, health impacts were reported at the time of the events. However, health impacts from heatwaves are often not reported while the event is ongoing; and even less severe heatwaves pose significant risks. In the next Section 1.2, we evaluate the extent to which the continent has been warmed by human-caused climate change. Section 2 then assesses the expected risks to human health associated not only with the most intense heatwave events but over the whole summer period.

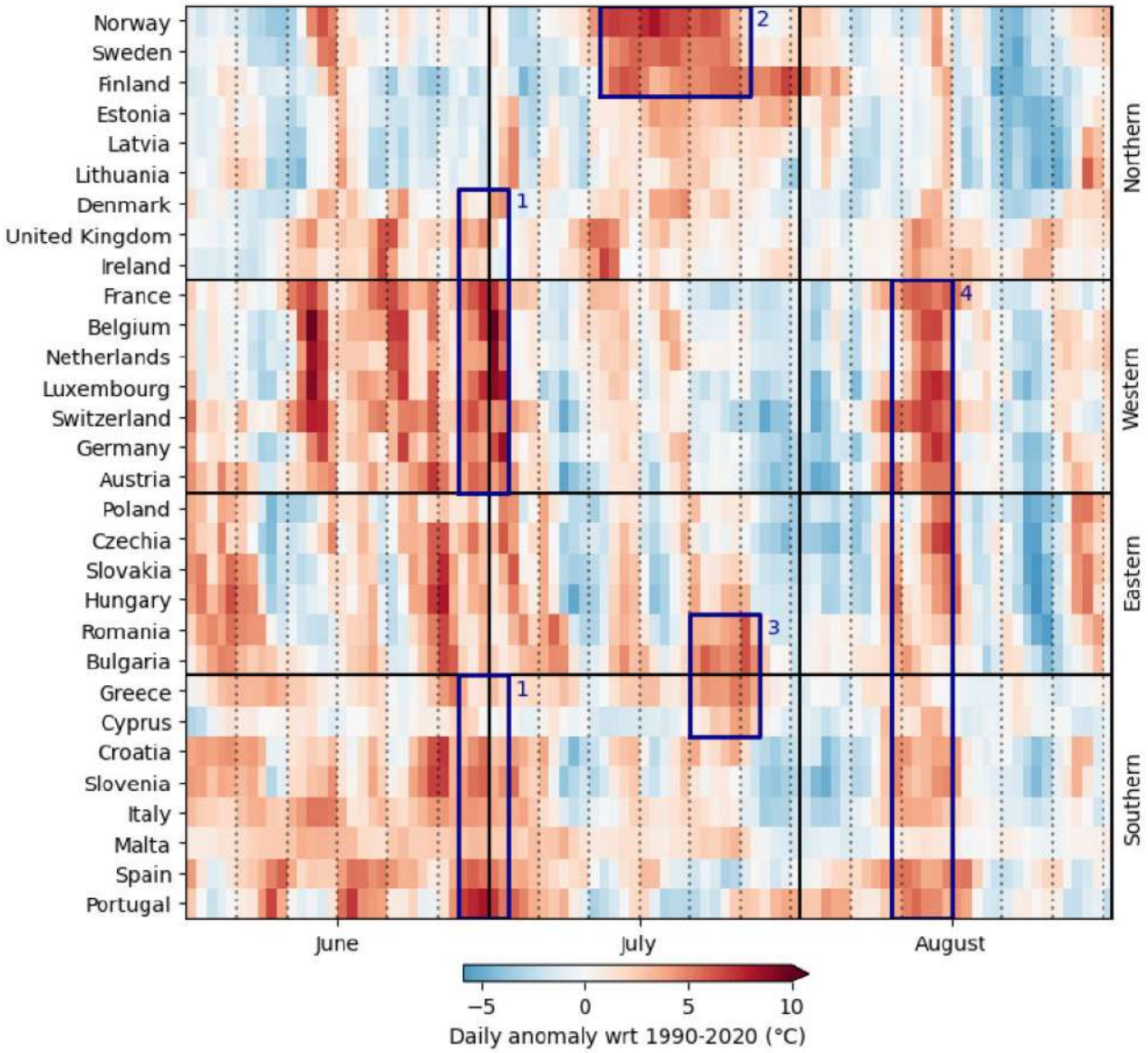

***Figure 4**: Daily mean temperature anomaly with respect to 1990-2020 daily climatology, averaged across all grid cells within the country bounded by the domain 11W, 35E; 33N, 66N (ERA5). Dark blue boxes highlight periods of particularly dangerous heat that have previously been the subject of attribution studies (see text for details).*

1.2 Changes in monthly mean temperatures

To understand the extent to which summer temperatures across Europe have been affected by human-caused climate change, we use an established probabilistic attribution protocol (Philip et al., 2020). The long-term trend in global mean temperatures is known to be fully driven by human activity, leaving the climate in 2025 an estimated 1.3°C warmer than it would have been without this anthropogenic warming. We use a statistical model to represent the relationship between monthly mean temperatures in each location and global mean temperatures, and so to describe the effect of this human-caused warming on local temperatures. Historic trends in temperatures are assessed in two observation-based gridded datasets, along with trends in the output of 38 climate models from

the most recent CMIP6 experiments (Table A2). For each of these sources we estimate the local change in temperature associated with 1.3°C of warming, and finally combine the results into a single estimate known as the synthesis (Otto et al., 2024). This process is repeated for each of the boreal summer months (June, July and August) and in each of the 854 cities. A more detailed description of the datasets and methods used can be found in Section 3.1. Full uncertainty ranges were also obtained for each city and month via bootstrapping, for use in the mortality attribution analysis described in the next section, but are not presented in detail here; all ranges reported in the text are ranges of estimated changes across all cities within each country or region.

The results presented here use the synthesised change in temperatures, taking into account both historical trends and simulations from global climate models. This reduces the uncertainty in observed trends, which can be high; however, observed warming trends across Europe in recent decades are typically somewhat stronger than those simulated by climate models, so the temperature increases reported here should be taken as a conservative estimate of the true warming that people are experiencing across the continent. This is discussed in more detail in section 3.3.2.

Figure 5 shows the spatial pattern of the synthesised changes in summer temperatures across Europe, along with the mean change per month in across all of the cities in each country; maps of the synthesised change in each month can be found in the Appendix in Figure A1, and a table including the range of estimates within each country in Table 1.

Over Europe as a whole there is a northwest-southeast gradient, with central, southern and eastern Europe warming substantially more than countries in the northern region. Warming also tends to be stronger further inland, with the lowest estimated rates of warming recorded in Ireland, Cyprus, Malta and Portugal, countries where all of the cities in the study are in coastal regions. On average the 854 cities have warmed by an estimated 1.9°C in June (range of estimates: 0.8 to 3.3°C); 2.2°C in July (0.7 to 3.5°C), and 2.3°C in August (0.9 to 3.6°C). In 825 of the 854 cities (97%) summer temperatures have warmed by more than 1.5°C on average; in 569 of the 854 cities (67%), by more than 2°C; and 132 cities (15%), by more than 2.5°C. These results are entirely consistent with the findings of previous attribution studies across Europe, where temperatures are known to be warming more rapidly than the global mean (Copernicus, 2024).

***Table 1**: Mean summer temperature and anomaly with respect to 1990-2020, averaged over all land grid cells in ERA5 in the country and within each domain 11W, 35E; 33N, 66N (shown in Figure 1). 'Attributable change in intensity' is the average of the synthesised change in temperatures taking into account trends in both observational data products (ERA5 and E-Obs) and climate models from June-August over all cities and months, with the range of the estimated changes given in brackets.*

Region	Country	# cities	Mean JJA temperature (°C)	Mean JJA anomaly (°C)	Synthesised change in JJA (°C)
Northern	Norway	4	13.04	0.88	1.7 (1.4 - 2.2)
	Sweden	14	14.92	0.63	1.8 (1.2 - 2.1)
	Finland	9	15.65	0.51	1.9 (1.5 - 2.2)
	Estonia	3	16.40	-0.08	2.0 (1.6 - 2.2)
	Latvia	10	16.50	-0.26	2.0 (1.5 - 2.2)
	Lithuania	6	16.86	-0.34	2.0 (1.5 - 2.3)
	Denmark	4	16.65	0.47	1.6 (1.1 - 2.0)
	United Kingdom	135	16.10	1.49	1.8 (1.1 - 2.4)
	Ireland	5	15.63	1.19	1.1 (0.7 - 1.5)
Western	France	72	20.40	1.56	2.3 (1.4 - 3.3)
	Belgium	15	18.70	1.38	2.1 (1.5 - 2.5)
	Netherlands	47	18.39	1.10	2.0 (1.6 - 2.5)
	Luxembourg	1	18.33	0.97	2.3 (2.2 - 2.5)
	Switzerland	12	15.76	1.49	2.6 (2.0 - 3.2)
	Germany	127	18.41	0.78	2.2 (1.4 - 2.8)
	Austria	6	16.99	1.03	2.6 (1.9 - 2.9)
Eastern	Poland	68	18.26	0.14	2.2 (1.5 - 3.0)
	Czechia	18	18.23	0.48	2.4 (1.8 - 3.1)
	Slovakia	8	19.01	0.65	2.6 (1.9 - 3.2)
	Hungary	19	22.30	0.89	2.4 (1.8 - 3.0)
	Romania	35	21.51	1.26	2.6 (1.8 - 3.5)
	Bulgaria	18	23.13	1.72	2.4 (1.7 - 2.9)
Southern	Greece	14	25.09	1.43	2.0 (1.1 - 2.6)
	Cyprus	3	27.74	0.16	1.5 (1.4 - 1.6)
	Croatia	7	22.75	1.22	2.5 (2.0 - 3.0)
	Slovenia	2	20.47	0.97	2.7 (2.1 - 3.2)
	Italy	87	22.87	1.31	2.4 (1.4 - 3.5)
	Malta	1	25.84	1.34	1.6 (1.6 - 1.7)
	Spain	90	24.11	1.87	2.2 (1.3 - 3.6)
	Portugal	14	23.41	1.72	1.5 (0.9 - 2.2)

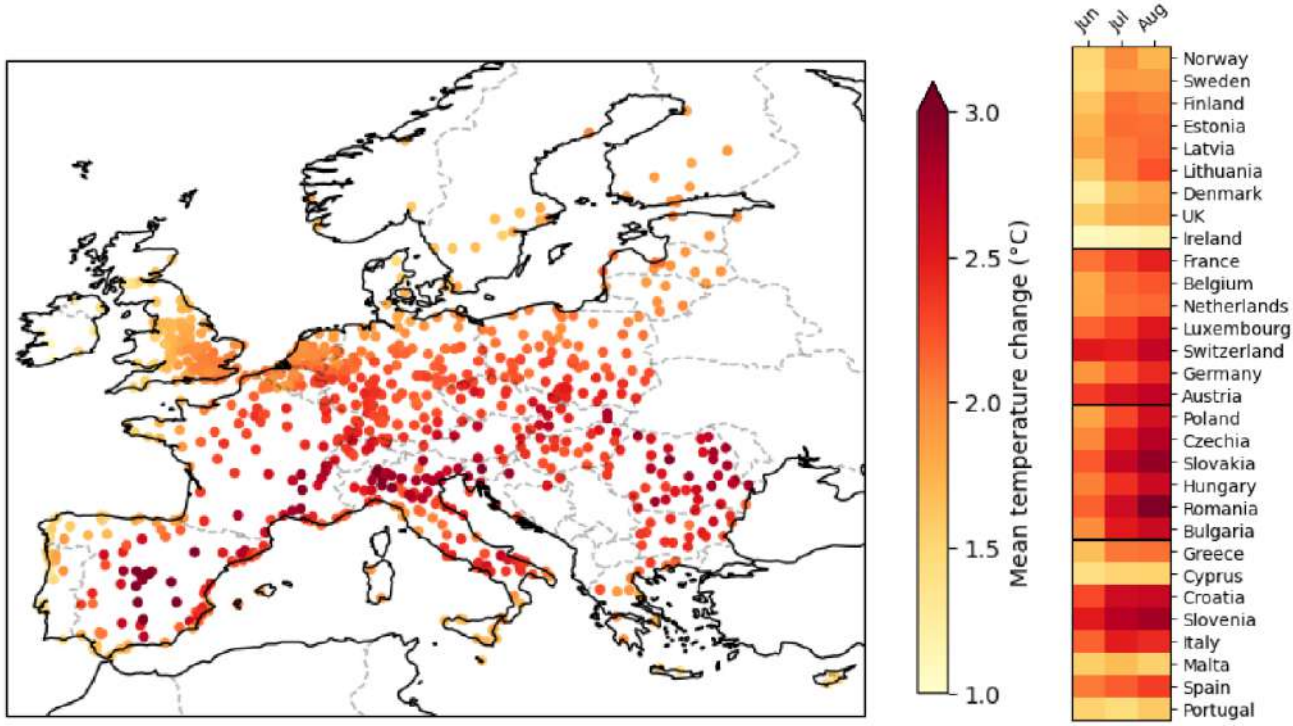

***Figure 5**: (left) Map of synthesised change in summer temperatures averaged over June, July and August and (right) panel plot showing the mean of the estimated changes in each country in each month.*

2 Health impacts of changing summer temperatures

In this section, we use established exposure-response relationships (Masselot et al., 2023) to estimate the excess mortality given the observed temperatures (the 'factual' scenario) and also under the counterfactual scenario of a 1.3°C cooler world. To calculate the exposure response relationships, we used historical mortality data (1990-2019), and an established three-step methodological framework that accounts for lagged effects and addresses data sparsity through pooled estimates and extrapolation techniques (Masselot et al., 2023). The factual temperatures are the daily mean temperatures in each city in the ERA5 reanalysis (Hersbach et al., 2020), and the counterfactuals are calculated by subtracting the synthesised change in temperatures in each city associated with 1.3°C of warming since the preindustrial period, as discussed in section 1.2. By comparing these estimates, we calculate how many more people are expected to have died in each city during the summer of 2025 due to the excess heat caused by anthropogenic warming.

2.1 Overall results

Overall, we found 24,404 (95% empirical Confidence Intervals: 21,968 to 26,806) excess deaths due to heat during summer 2025, with 68% (64% to 71%) estimated to be attributable to human-

induced climate change (Table 2). Older populations are affected the most, with more than 80% of the excess heat-related deaths occurring among people older than 65 years.

***Table 2**: Population figures, median and 95% empirical confidence intervals for estimated excess heat-related deaths presented as crude numbers and rates per 1 million population for deaths attributable to heat, number of deaths attributable to human-induced climate change and proportion of excess heat-related deaths that can be attributed to human-induced climate change. Note that a minor rounding error occurs when summing the crude numbers by age group, resulting in a slight difference from the overall total.*

Age group	Population	Excess deaths	Rate per 1 million population	Attributable to climate change	Proportion of excess deaths due to climate change
Total	158,473,649	24404 (21968, 26806)	154 (139, 169)	16496 (15013, 17864)	0.68 (0.64, 0.71)
20-44	66,886,597	608 (434, 795)	9 (6, 12)	279 (208, 352)	0.46 (0.36, 0.57)
45-64	54,059,644	3058 (2557, 3593)	57 (47, 66)	1866 (1589, 2133)	0.61 (0.55, 0.67)
65-74	19,676,737	3738 (3279, 4171)	190 (167, 212)	2487 (2210, 2738)	0.67 (0.63, 0.7)
75-84	12,762,858	7019 (6305, 7726)	550 (494, 605)	4835 (4408, 5250)	0.69 (0.66, 0.72)
85+	5,087,812	9959 (9012, 10964)	1957 (1771, 2155)	7028 (6397, 7657)	0.71 (0.67, 0.73)

2.2 Spatial variation

To allow comparison between cities across Europe, accounting for the different age distributions among populations, we calculate the age-standardised excess mortality. Briefly, the excess deaths were first converted into age-specific mortality rates by dividing by the corresponding population. Standardised rates for each city are then weighted averages of these rates, using the 2013 European standard population as the weighing reference. The geographical distribution of the median age-strandardised excess mortality and the median proportion of heat-related deaths estimated to be attributed to human-induced climate change are shown in Figure 6. When assessing the spatial distribution of the median age-standardised excess mortality in the 854 cities in Europe, there is a north to south gradient, with cities in southern and southeast Europe affected the most, where summer temperature anomalies were highest (Figure 2). Although the excess mortality rates are lower in northern Europe, mainly because temperatures were lower, the proportion of deaths attributable to climate change is higher. This spatial pattern closely reflects the distribution of changes in Figure 5.

When aggregating the available cities at the country level, we found the highest age-standardised excess mortality due to heat in Croatia (382; 289 to 469), Greece (380; 312 to 442), and Bulgaria (371; 267 to 477) (Table A1). The countries most affected by human-induced climate change, in relative terms, were Sweden, Malta, and Slovakia, where 83% of the estimated heat-related deaths were found to be attributable to climate change (Table A1).

When examining the 30 available European capitals, we estimated that Rome, Athens and Bucharest had the highest standardised excess mortality per 1 million population (Table 3). In absolute terms, we estimated 835 (712 to 938) heat-related deaths that could be attributable to climate change in Rome, 630 (541 to 717) in Athens and 409 (310 to 511) in Paris. In relative terms, the largest proportion of heat-related deaths due to climate change was observed in Stockholm (97%; 91% to 98%), Madrid (93%; 76% to 98%) and Bratislava (85%; 70% to 93%).

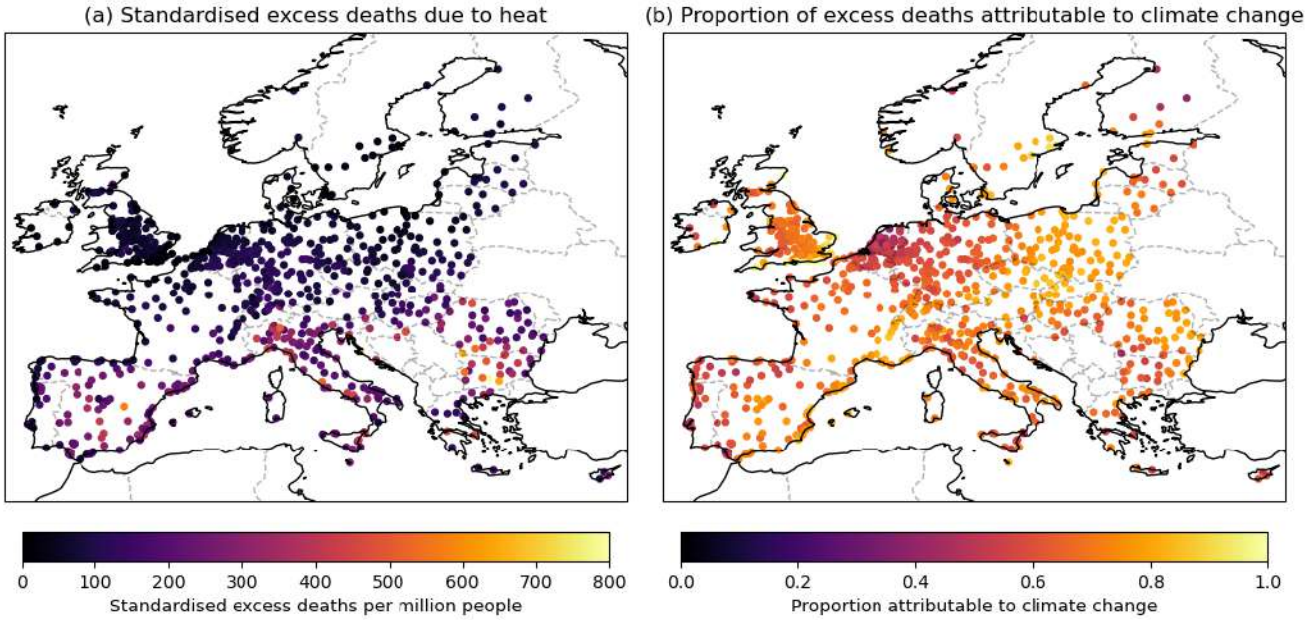

***Figure 6**: Maps of median standardised excess mortality per million people and median proportion of mortality attributed to climate change by city.*

***Table 3**: City specific population figures (based on the capitals), median and 95% empirical confidence intervals for excess heat-related presented as crude numbers, age-standardised rates (using the 2013 European standard population) per 1 million population, number of deaths attributable to human-induced climate change and proportion of excess heat-related deaths that can be attributed to human-induced climate change. The numbers reflect the heat-related impacts during the entire summer of 2025.*

Capital	Population	Excess deaths	Standardised excess mortality per million	Attributable to climate change	Proportion of excess deaths due to climate change
Paris	6,869,559	582 (433, 754)	95 (71, 123)	409 (310, 511)	0.70 (0.60, 0.73)
London	5,894,656	458 (302, 600)	114 (76, 149)	315 (215, 403)	0.69 (0.67, 0.71)
Madrid	2,871,466	423 (298, 574)	148 (104, 202)	387 (268, 497)	0.93 (0.76, 0.98)
Berlin	2,805,374	219 (174, 293)	82 (66, 110)	140 (115, 164)	0.66 (0.52, 0.69)
Athens	2,269,492	1093 (905, 1274)	470 (389, 548)	630 (541, 717)	0.58 (0.52, 0.63)
Rome	2,158,892	1280 (1135, 1432)	532 (472, 596)	835 (712, 938)	0.65 (0.59, 0.70)
Bucharest	1,665,377	472 (359, 609)	352 (269, 452)	360 (282, 442)	0.76 (0.69, 0.81)
Lisbon	1,425,616	84 (62, 121)	56 (41, 80)	50 (40, 67)	0.60 (0.55, 0.66)
Budapest	1,414,149	142 (85, 230)	106 (63, 173)	111 (71, 163)	0.79 (0.69, 0.86)
Warsaw	1,381,256	83 (51, 128)	60 (37, 93)	68 (43, 97)	0.82 (0.74, 0.87)
Vienna	1,315,748	111 (76, 160)	96 (66, 139)	86 (63, 112)	0.77 (0.67, 0.84)
Stockholm	1,142,160	31 (18, 45)	33 (18, 47)	30 (17, 42)	0.97 (0.91, 0.98)
Prague	990,604	46 (26, 73)	53 (31, 84)	36 (22, 54)	0.80 (0.71, 0.85)
Sofia	950,740	164 (106, 240)	214 (138, 311)	120 (81, 161)	0.72 (0.64, 0.80)
Dublin	893,653	10 (4, 17)	18 (7, 30)	8 (3, 13)	0.75 (0.73, 0.79)
Brussels	808,139	84 (66, 106)	125 (98, 159)	50 (40, 59)	0.60 (0.52, 0.63)
Zagreb	630,723	201 (138, 257)	348 (241, 444)	139 (104, 171)	0.69 (0.64, 0.77)
Amsterdam	616,727	41 (30, 68)	88 (66, 141)	20 (16, 26)	0.49 (0.30, 0.65)
Riga	550,511	45 (9, 95)	81 (15, 172)	31 (7, 57)	0.67 (0.54, 0.94)
Helsinki	453,721	27 (15, 39)	74 (42, 105)	22 (13, 31)	0.80 (0.75, 0.83)
Oslo	435,270	26 (7, 43)	88 (24, 142)	15 (5, 23)	0.55 (0.38, 0.71)
Vilnius	429,750	31 (5, 75)	79 (14, 197)	20 (2, 45)	0.68 (0.19, 0.93)

Copenhagen	415,428	9 (5, 14)	25 (14, 40)	7 (4, 11)	0.82 (0.75, 0.87)
Bratislava	337,865	18 (9, 32)	68 (37, 123)	15 (8, 24)	0.85 (0.70, 0.93)
Tallinn	316,478	15 (5, 24)	52 (19, 86)	11 (4, 17)	0.77 (0.50, 0.9)
Ljubljana	217,685	35 (24, 46)	170 (116, 227)	26 (19, 34)	0.76 (0.70, 0.83)
Bern	176,221	54 (39, 66)	282 (203, 349)	33 (24, 41)	0.63 (0.51, 0.68)
Nicosia	171,474	16 (10, 21)	126 (81, 170)	10 (7, 12)	0.60 (0.56, 0.65)
Valletta	170,361	36 (25, 47)	256 (184, 337)	30 (22, 37)	0.83 (0.77, 0.89)
Luxembourg	70,074	7 (5, 9)	119 (88, 150)	4 (3, 5)	0.60 (0.48, 0.67)

2.3 Temporal variation

The top panel of Figure 7 shows the daily variation of the excess heat-related deaths under the factual and counterfactual scenario across Europe over the summer. These results are based on an aggregation of the 854 cities. The highest number of excess deaths is observed during the late June - early July heatwave, whereas the second worst period was during the second week of August. These two events correspond to the heat events labelled as ‘box 1’ and ‘box 4’ in Figure 4; the daily estimates of the standardised excess deaths in cities of over 50,000 people in each country are shown in Figure 8, with the same boxes overlaid for reference. As a result, the region with the largest estimated numbers is western Europe, driven mainly by the extreme early heatwave (Figure 7, lower left panel).

The effect of the Fennoscandia heatwave (Figure 8, box 2), although extremely impactful across the affected countries as a whole (Barnes et al., 2025), led to only a moderate increase in health risks in the large cities included in this study; however, as noted in section 1.1, the highest temperatures were reported in the northern parts of the country, which are not represented in this sample, and therefore the true risk is probably under-represented here.

The heatwave across the Balkans (Figure 8, box 3), which was associated with devastating wildfires across the region, was associated with the highest daily risks of any of the events, with an average of 10 additional deaths per million population across the seven-day period affected. Again, this is almost certainly an underestimate of the true mortality during this event, because six Balkan countries that fall outside of the scope of this study experienced very similar temperatures during this period. Despite the relatively small spatial extent of this heatwave, the resulting increase in mortality is clearly visible in the Europe-wide totals in Figure 7.

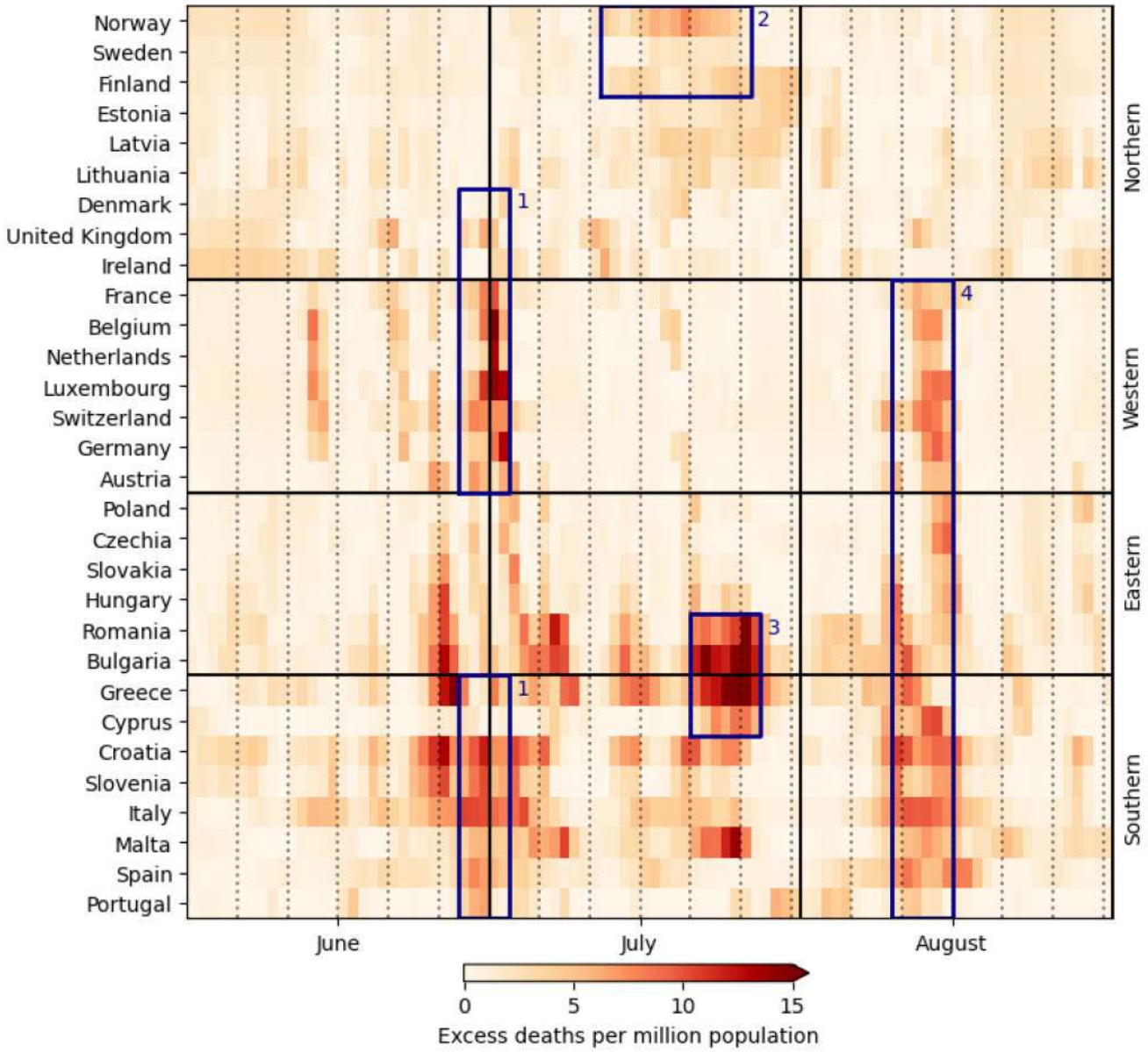

***Figure 7**: Standardised excess deaths per million population, aggregated over all countries. Dark blue boxes highlight periods of particularly dangerous heat that have previously been the subject of attribution studies (see section 1.1 for details).*

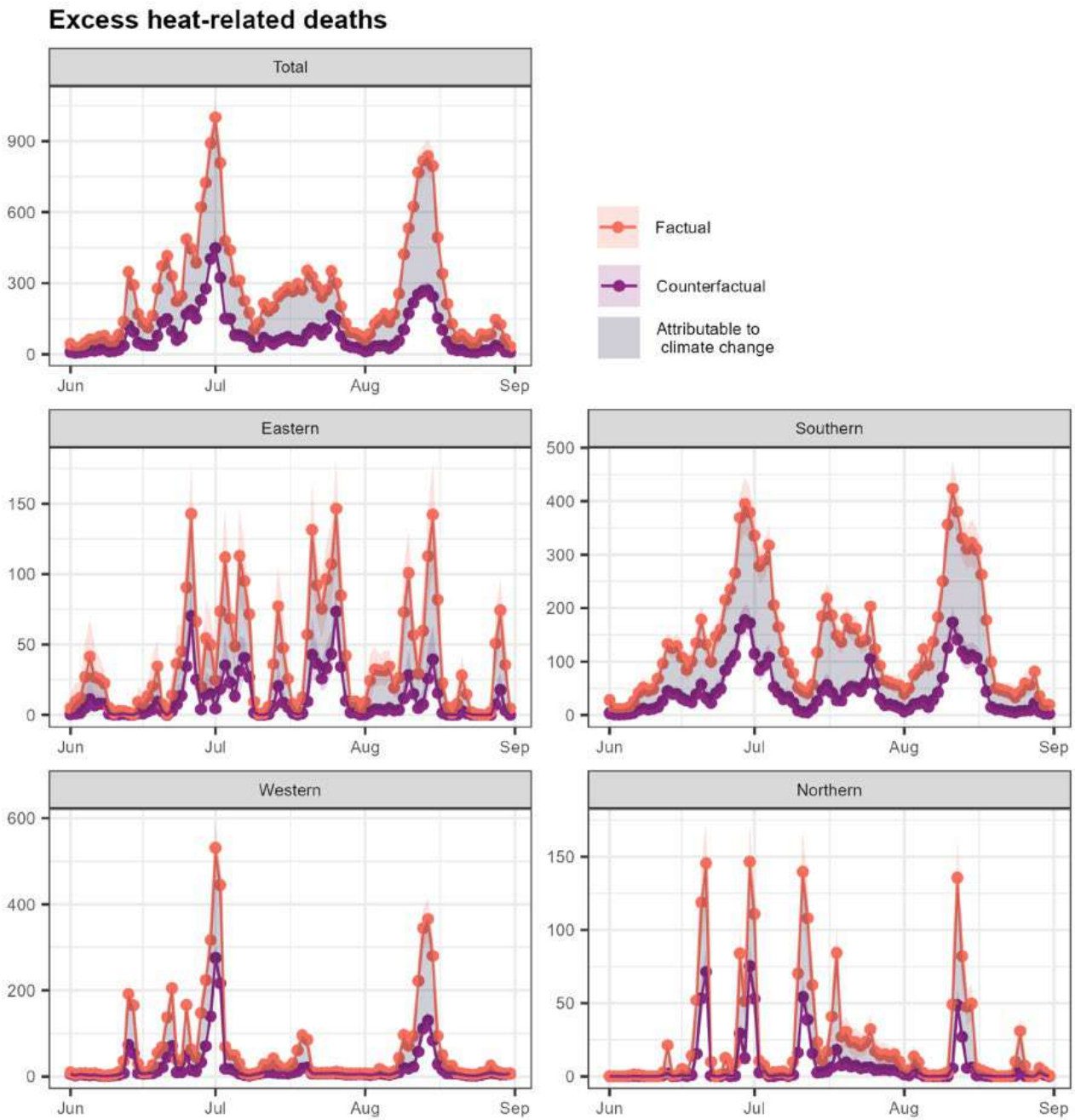

Figure 8: *Median estimates and 95% empirical confidence intervals of heat-related deaths under factual and counterfactual temperature scenarios for the whole Europe and 4 major European regions (eastern, southern, western and northern). The grey shaded area represents the estimated number of heat-related deaths attributed to human-induced climate change. Note that the estimates in this figure are based on aggregating the results of the 854 cities.*

2.4 Comparison of results with previous literature

A study in Europe estimated that more than 60,000 people across Europe died from heat during summer 2022 (Ballester et al., 2023). The same population and methods were used to estimate heat-related deaths during the less intensely hot summer of 2023, reporting over 47,000 heat-related deaths (Gallo et al., 2024). In our analysis, we report around 24,000 deaths across a

population of 158 million, approximately 30% of the 534 million population considered in that study, placing our estimates in line with those of summer 2022. Our approach is also comparable with another study focusing on the same 854 cities (Masselot et al., 2023), which reported an average of 13,589 deaths (11,530 to 15,475) between 1990 and 2019. Our estimate is about 10,000 heat-related deaths higher, reflecting the much warmer summer of 2025 compared to the period covered by that study.

Our study is also comparable with studies examining the proportion of heat-related deaths attributed to human-induced climate change. A study on Europe focusing on summer 2022 found that more than 50% of the excess deaths could be attributed to human-induced climate change (Beck et al., 2024). A global study recently showed that more than 50% of the reported heatwave-related deaths could be attributable to climate change (Hundessa et al., 2025). Our results suggest that 68% of the observed heat-related deaths could be attributed to climate change. This discrepancy may reflect differences in event definition, climate attribution approaches, as well as the fact that our study focuses on urban populations, which generally experience greater warming (Tuholske et al., 2021). Our results are comparable with our previous rapid attribution analysis in 12 European cities, which reported almost 65% of the observed excess deaths to be attributed to human-induced climate change.

3 Data & methods

3.1 Data and methods used in temperature attribution

In section 1 of this report, we study the influence of anthropogenic climate change on average summer temperatures by comparing the likelihood and intensity of similar weather conditions at present with those in a 1.3°C cooler climate representing the preindustrial past (1850-1900, based on the Global Warming Index). The data and methods used in this section are described in detail below.

3.1.1 Observational datasets

The 'observed' temperatures for each city are extracted from the gridded datasets by selecting the closest grid cell to the coordinates of the city.

The observational datasets used are as follows:

- **ERA5** - The European Centre for Medium-Range Weather Forecasts's 5th generation reanalysis product, ERA5, is a gridded dataset that combines historical observations into global estimates using advanced modelling and data assimilation systems (Hersbach et al., 2020). We use daily mean temperature data from the ERA5 product at a resolution of 0.25° × 0.25°, from January 1950 until the end of August 2025.

- **E-OBS (v31.0e + pre1950)** - This is a gridded land-only dataset covering Europe, derived from the interpolation of station-derived meteorological observations (Cornes et al., 2018). We use daily mean temperature data from this product at a resolution of 0.25° × 0.25°, from January 1920 to June 30th 2025. For three locations no data were available because the nearest grid cell is not designated as land. For all other stations in the study, at least 62 complete summers of mean daily temperatures were used to construct the monthly time series.

As a measure of anthropogenic climate change we use the global mean surface temperature (GMST), where GMST is taken from the National Aeronautics and Space Administration (NASA) Goddard Institute for Space Science (GISS) surface temperature analysis (GISTEMP, Hansen et al., 2010 and Lenssen et al. 2019). To reduce variability in the GMST due to the El Nino-Southern Oscillation (ENSO), we use a four-year rolling average of the GMST, centred on the third year.

3.1.2 Climate models

In the attribution step we use a multi-model ensemble of coupled global circulation models from the CMIP6 experiments (Eyring et al., 2016). For all simulations, the period 1850 to 2014 is based on historical simulations, while the SSP5-8.5 scenario is used to project from 2015 to 2030. All years from 1850 to 2030 were used to estimate the historic warming trend. 38 models were used in the analysis, each providing one realisation to the multi-model ensemble. In an exploratory analysis comparing the spatial climatology of summer temperatures from 1990-2020 with the observed climatology, all models were found to perform relatively well. To avoid using different subsets of climate models in each region, no further selection was carried out based on the local seasonal cycles or parameter fits. However, five model variants were removed from the original ensemble of 43, because they were lower-resolution variants of other models within the ensemble. Details of the 38 models included in the study can be found in Table A2 in the Appendix.

3.1.3 Statistical modelling of trends

Methods for observational and model analysis, and for synthesis of the results, are used according to the World Weather Attribution Protocol, described in Philip et al., (2020), with supporting details found in van Oldenborgh et al., (2021), Ciavarella et al., (2021), Otto et al., (2024) and here. The key steps, presented in section 1, are: trend estimation from observations; attribution using climate models; and synthesis of the attributable change in temperature.

The attribution analysis is carried out independently for each dataset, city and calendar month (June, July and August). We first extract the time series of monthly mean temperatures by selecting the grid cell closest to the coordinates of the city. For each time series we estimate the parameters of a nonstationary normal distribution in which the mean monthly temperature depends linearly on GMST, while the variance remains stationary. This statistical model is then used to estimate the expected change in mean temperature associated with a 1.3°C reduction in GMST, corresponding to the expected difference in temperature between the current climate and a 1.3°C cooler

counterfactual climate representing the preindustrial past (1850-1900, based on the Global Warming Index). 95% confidence intervals are obtained by bootstrapping, using a sample size of 1000.

3.1.4 Synthesis of trends

For a given city and calendar month, the estimated change in intensity from the observational products and climate models are combined into a single result using WWA's standard synthesis algorithm (Otto et al., 2024). First, the results from observations are averaged, with a representation error added in quadrature to reflect any difference in mean trend; the results from climate models are combined into a separate precision-weighted average, with a term added in quadrature to account for inter-model spread as well as internal variability. These two weighted averages are then again combined using inverse-variance (precision) weighting, to obtain an overall best estimate and estimated upper and lower bounds of a 95% confidence interval.

3.1.5 Calculating counterfactuals

Factual daily mean temperatures for June-August 2025 were taken from ERA5 reanalysis (E-Obs data were not available for August at the time of writing). The preindustrial counterfactual was obtained by subtracting the best estimate of the synthesised change in intensity for that day's calendar month from the factual temperature, and lower and upper confidence bounds by subtracting the upper and lower bounds of the synthesised change, respectively. These three counterfactual temperatures were used as inputs to the epidemiological model, along with the factual temperatures, to estimate the change in mortality attributable to the synthesised change in monthly mean temperatures.

3.2 Data & methods used in mortality attribution

To estimate heat-mortality attributable to human-induced climate change, we applied a framework that combines exposure-response functions with temperature time series under factual and counterfactual scenarios. The method comprises three key steps:

1. **Deriving exposure-response functions**: We obtained age-specific temperature–mortality relationships for the 854 cities in Europe from Masselot, et. al., 2023 (freely available here).
2. **Estimating heat-related mortality**: These relationships were used to calculate excess deaths under both factual and counterfactual temperature scenarios (see previous section).
3. **Attributing deaths to climate change**: The comparison (absolute or relative difference) between excess deaths in the factual and counterfactual scenarios quantifies the impact of human-induced climate change on mortality.

Step 1: Exposure-response functions were derived from daily mortality data from the Multi-country Multi-city Collaborative Research Network (MCC; https://mccstudy.lshtm.ac.uk/), annual Eurostat statistics, and additional city-specific data from sources including satellite observations (MODIS, Copernicus). Daily mean temperatures came from the ERA5-Land reanalysis dataset for 1990–

2019. The associations were stratified by age group (20–44, 45–64, 65–74, 75–84, 85+) and city, capturing variations in vulnerability. This framework also applies pooling of the estimates, providing robust curves in cities where data is sparse (Masselot, et. al., 2023). Figure 9 shows the relative risk curves in the 30 European capitals available in the study.

Step 2: Relative risks were calculated for both factual and counterfactual temperatures and converted into heat-related mortality fractions following Vicedo-Cabrera et al. (2023) and Beck et al. (2024), accounting for lagged effects of heat. Daily deaths during the heatwave were estimated assuming a constant rate based on historical Eurostat data (Masselot, et. al., 2023). Multiplying this rate by the attributable mortality fraction yielded excess deaths in each scenario. As the interest was in estimating the impact of heat, relative risks were derived from the temperature–mortality curve focusing on temperatures above the minimum mortality temperature (MMT).

Step 3: Finally, the difference between excess deaths in the factual and counterfactual scenarios provides the number of heat-related deaths attributable to anthropogenic climate change. We also calculated the proportion of heat-related deaths in the factual scenario attributable specifically to human-induced climate change (Beck et al., 2024).

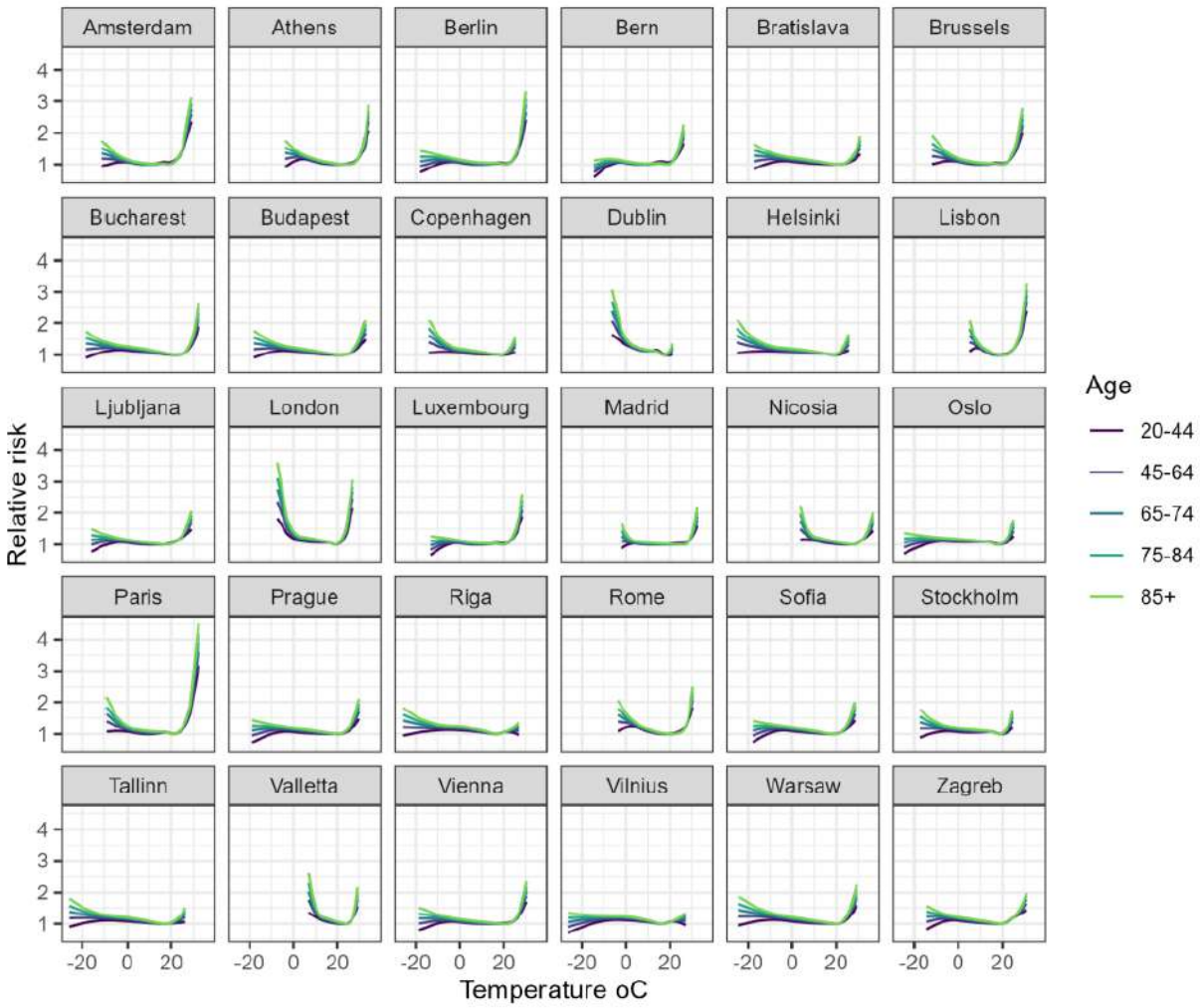

***Figure 9**: Mean temperature-related relative mortality risk across the 30 European capitals by age group, as retrieved from Masselot et al., 2023.*

3.3 Limitations of the methods and sensitivity analyses

The rapid nature of this type of study precluded access to observed death counts across the 854 European cities. To address this, we assumed a constant daily death rate at the optimum temperature in each city, based on historical annual mortality data. However, deaths typically peak during heatwaves, so the true death rate is likely higher than the constant rate used here, potentially leading to an underestimation of the absolute burden of heat. This limitation does not affect relative estimates, as these are independent of the underlying mortality rate.

While this study examines all-cause mortality, it does not account for other adverse health effects of heat, including impacts on mental health, hospital admissions, or medication use. The study also does not account for adaptation. As the exposure-response functions used in this study were derived using mortality data up to 2019, the results might not capture the potential temporal attenuation of the temperature effect which has been reported in previous literature (Vicedo-Cabrera et al., 2018). Indeed, improved adaptation policies and infrastructure (Vicedo-Cabrera et al., 2018) and autonomous adaptation measures addressing the increasing burden of heat have the potential to reduce vulnerabilities and impacts. In addition to this, our study does not capture the changes in the baseline population that occurred post COVID-19. Not accounting for this might lead to higher numbers in some cities.

We also note that temperatures in the cities may not be representative of the temperatures across the whole country, so can't extrapolate beyond the geographic scope of the study - this is particularly the case in Scandinavia, where the cities are all in the south, while the hottest temperatures were recorded further north. Furthermore, climate models are known to underestimate the rate of warming across much of Europe (eg. Vautard et al., 2023) and so the estimated changes in temperatures attributable to anthropogenic warming may themselves be conservative estimates; the sensitivity of the analysis to this is considered in section 3.3.2 below.

3.3.1 Sensitivity to non-optimum temperatures

The main analysis focuses on temperatures above the MMT, excluding deaths from colder summer temperatures. Table 4 extends the analysis to the full temperature-mortality curve. This increases the total number of deaths due to non-optimal temperatures to 28,742 (26,311 to 31,089), as it also includes cold-related mortality. In contrast, deaths attributable to human-induced climate change are lower, 11,827 (10,091 to 13,438), nearly 5,000 fewer, but still substantial. The proportion attributable to climate change remains high at 40% (36% to 46%). This reduction reflects a protective effect in some regions, particularly northern Europe, where warming has lessened risks from colder summer temperatures.

***Table 4**: Population figures, median and 95% empirical confidence intervals for excess mortality related to non-optimal temperature presented as crude numbers and rates per 1 million population for deaths attributable to heat, number of deaths attributable to human-induced climate change and proportion of excess heat-related deaths that can be attributed to human-induced climate*

change. Note that a minor rounding error occurs when summing the crude numbers by age group, resulting in a slight difference from the overall total.

Age group	Population	Excess deaths	Rate per 1 million population	Attributable to climate change	Proportion of excess deaths due to climate change
Total	158,473,649	28742 (26311, 31089)	181 (166, 196)	11827 (10091, 13438)	0.41 (0.36, 0.46)
20-44	66,886,597	705 (572, 864)	11 (9, 13)	212 (119, 302)	0.30 (0.19, 0.39)
45-64	54,059,644	3547 (3111, 3978)	66 (58, 74)	1410 (1095, 1733)	0.40 (0.33, 0.46)
65-74	19,676,737	4426 (3979, 4829)	225 (202, 245)	1785 (1465, 2085)	0.40 (0.35, 0.46)
75-84	12,762,858	8264 (7555, 8985)	647 (592, 704)	3486 (2973, 3941)	0.42 (0.37, 0.47)
85+	5,087,812	11785 (10824, 12830)	2316 (2127, 2522)	4960 (4159, 5687)	0.42 (0.36, 0.47)

3.3.2 Sensitivity to strength of temperature trend

It is likely that the synthesised changes in temperature presented in section 1.2 represent a conservative estimate of the true level of warming in many regions across Europe.. Figure 10 shows a map of the historical change in temperatures in the 854 cities associated with 1.3°C of warming, obtained by averaging the change estimated from two observational datasets: ERA5 (reanalysis data based on a forecasting model, from 1950-2025) and E-Obs (interpolated from observations at weather stations, 1920-2024). Figure 6b shows the average warming simulated by 38 CMIP6 climate models, and figure 6c the difference between the two, highlighting where the underestimation is greatest. While the spatial pattern of warming across the continent is fairly similar in models and observations, the climate models fail to simulate the full range of observed changes: in observations, the monthly changes range from 0.16 to 5.1°C, and in the climate models, from 1.1 to 2.5°C (Figure 6d, with the distribution of observed changes in blue and modelled changes in red). This is particularly the case in June, which has the widest spread of observed changes and the narrowest spread of modelled changes, but is true of all months. The result of this is that for June temperatures, the synthesised changes (pink) are on average 0.8°C cooler than those actually observed (95% central interval of differences: -1.9°C to +0.3°C); for July, 0.4°C cooler (-1.3°C to +0.2°C); and for August, 0.5°C cooler (-1.3°C to +0.2°C). While some of this difference may be due to natural variability in the real world, previous studies have highlighted similar

discrepancies in climate models over Europe (eg. Vautard et al., 2023). The estimated temperature changes here should therefore be interpreted as a conservative estimate of the true level of human-caused warming across Europe.

To test the sensitivity of the mortality attribution to the choice of dataset, the analysis was run using not only the best estimate but also the upper and lower bounds of a 95% confidence interval for the change in each city and month, and repeated using trends estimated from observations only. The results of this analysis are shown in Table 5. Use of the observed temperature increases resulted in a larger number of heat-related deaths attributable to climate change, (18,825; 17,115 to 20,437), and a larger proportion (77%; 74% to 80%). Comparing these results to those shown in Table 1, we see that the lower bound of the number of attributable deaths when using observations only to estimate the trend overlap with the upper bound of the number of deaths when using the synthesised results.

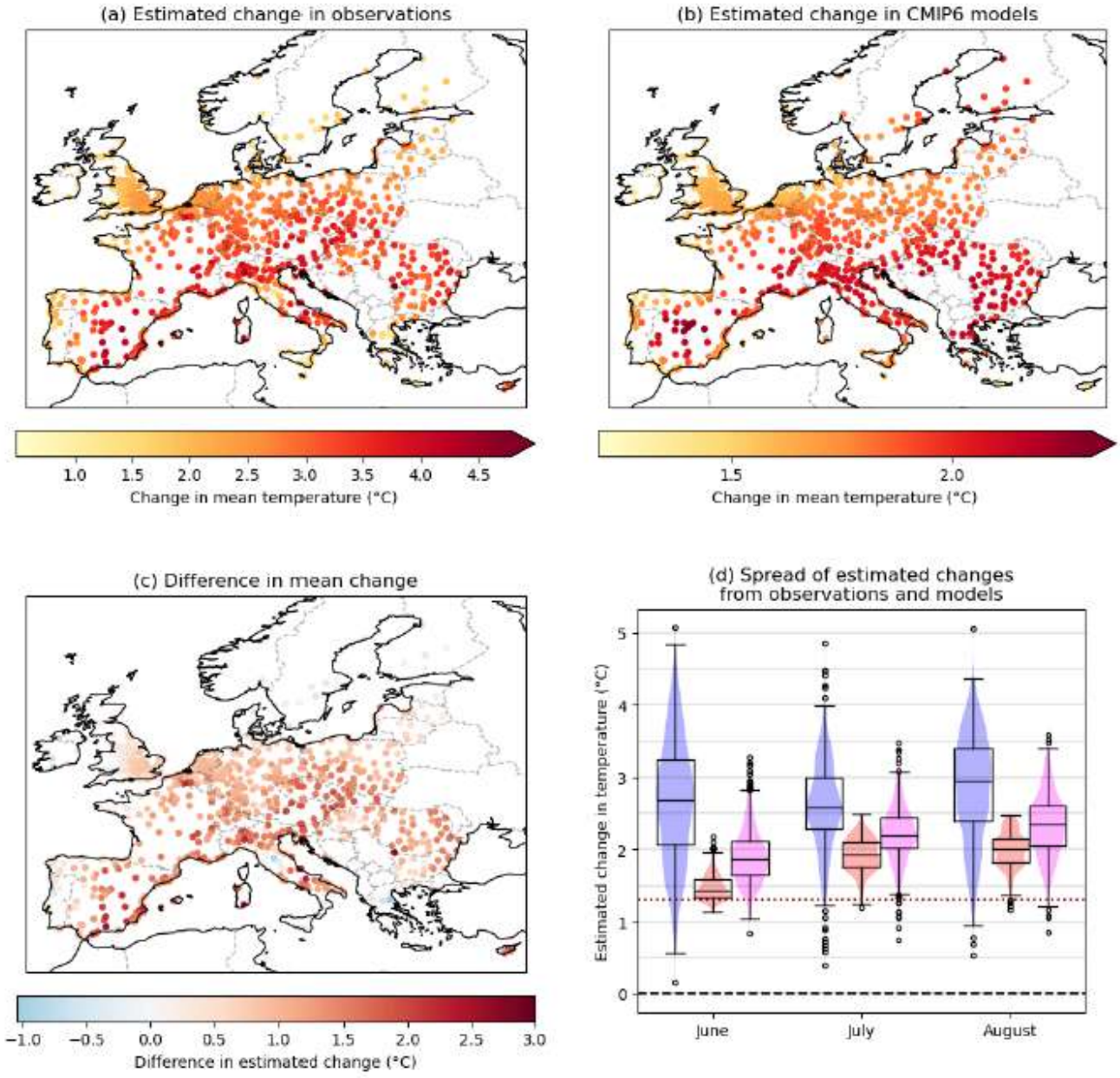

***Figure 10**: Maps of estimated change in summer temperatures in (a) observational data products and (b) CMIP6 climate models; (c) differences between the two data sources. (d) Boxplot and violinplots of the estimated changes each month across all cities, in observations (blue) and models (red), with synthesised change in pink. The box represents the central 50% of the distribution, the whiskers indicate points within 1.5 times the interquartile range of the box, and circles indicate points more extreme than this.*

***Table 5**: As Table 1, but using only observed changes in temperature to create the counterfactual daily temperatures, rather than the combined output of observations and climate models. Population figures, median and 95% empirical confidence intervals for excess mortality related to heat (temperatures higher than the minimum mortality temperature) presented as crude numbers and rates per 1 million population for deaths attributable to heat, number of deaths attributable to human-induced climate change and proportion of excess heat-related deaths that can be attributed to human-induced climate change. Note that a minor rounding error occurs when summing the crude numbers by age group, resulting in a slight difference from the overall total.*

Age group	**Population**	**Excess deaths**	**Rate per 1 million population**	**Attributable to climate change**	**Proportion of excess deaths due to climate change**
Total	158,473,649	24404 (21968, 26806)	154 (139, 169)	18825 (17115, 20437)	0.77 (0.74, 0.80)
20-44	66,886,597	608 (434, 795)	9 (6, 12)	328 (245, 415)	0.54 (0.44, 0.66)
45-64	54,059,644	3058 (2557, 3593)	57 (47, 66)	2150 (1833, 2458)	0.71 (0.64, 0.77)
65-74	19,676,737	3738 (3279, 4171)	190 (167, 212)	2839 (2528, 3122)	0.76 (0.72, 0.80)
75-84	12,762,858	7019 (6305, 7726)	550 (494, 605)	5505 (5011, 5982)	0.78 (0.75, 0.81)
85+	5,087,812	9959 (9012, 10964)	1957 (1771, 2155)	7993 (7276, 8717)	0.80 (0.77, 0.83)

Appendices

Figure A1: Synthesised change in temperatures per calendar month

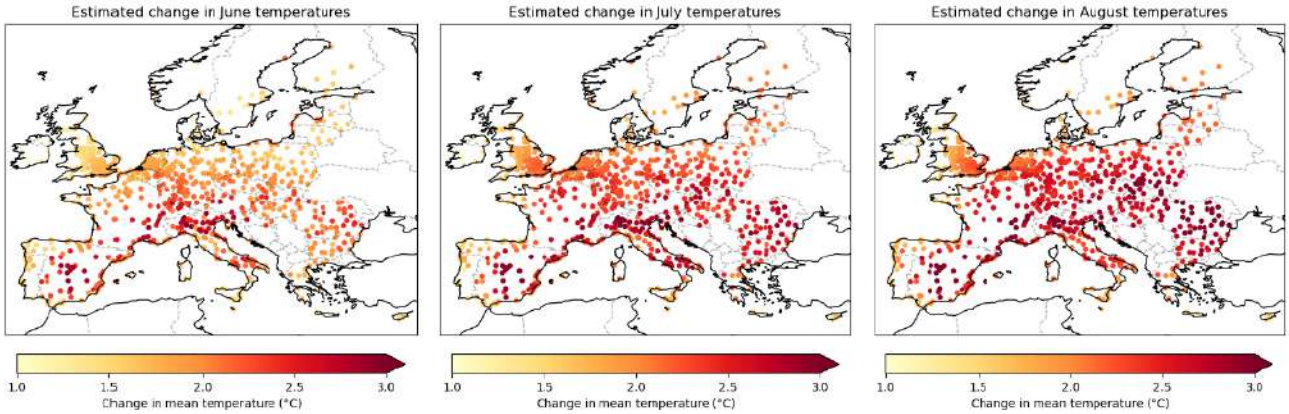

***Table A1**: Country specific population figures (based on the available cities per country), median and 95% empirical confidence intervals for excess heat-related presented as crude numbers, age-standardised rates (using the European standard population) per 1 million population, number of deaths attributable to human-induced climate change and proportion of excess heat-related deaths that can be attributed to human-induced climate change. The numbers reflect the heat-related impacts during the entire summer of 2025.*

Country	Population	Excess deaths	Standardised excess mortality per million	Attributable to climate change	Proportion of excess deaths due to climate change
United Kingdom	26,545,907	1687 (1303, 2045)	72 (56, 87)	1147 (900, 1384)	0.68 (0.67, 0.69)
Germany	23,406,685	2445 (2025, 2918)	101 (83, 121)	1477 (1245, 1701)	0.60 (0.54, 0.65)
France	17,962,199	2062 (1710, 2406)	110 (91, 129)	1444 (1224, 1661)	0.71 (0.66, 0.73)
Spain	17,714,878	3893 (3264, 4753)	207 (173, 253)	2841 (2374, 3310)	0.72 (0.65, 0.78)
Italy	17,186,805	6710 (5828, 7649)	335 (290, 382)	4597 (4083, 5137)	0.68 (0.64, 0.73)
Poland	10,396,899	694 (422, 1092)	75 (46, 117)	543 (353, 784)	0.78 (0.70, 0.85)
Romania	6,010,799	1487 (1031, 1954)	283 (198, 372)	1064 (767, 1342)	0.72 (0.66, 0.79)
Netherlands	5,644,325	411 (288, 665)	79 (56, 126)	200 (141, 257)	0.49 (0.29, 0.65)

Portugal	3,457,781	386 (314, 494)	108 (88, 138)	217 (180, 261)	0.56 (0.5, 0.61)
Greece	3,401,064	1372 (1127, 1597)	380 (312, 442)	808 (697, 913)	0.60 (0.54, 0.64)
Sweden	2,807,484	82 (49, 116)	30 (18, 43)	67 (41, 95)	0.83 (0.76, 0.87)
Hungary	2,806,295	362 (225, 552)	139 (87, 212)	266 (178, 366)	0.73 (0.65, 0.83)
Bulgaria	2,596,877	866 (620, 1115)	371 (267, 477)	552 (404, 683)	0.64 (0.57, 0.71)
Czechia	2,522,881	144 (88, 224)	66 (41, 102)	113 (71, 163)	0.79 (0.7, 0.84)
Belgium	2,455,390	269 (216, 324)	111 (89, 134)	154 (124, 182)	0.58 (0.50, 0.62)
Switzerland	1,977,029	280 (208, 355)	145 (107, 184)	207 (154, 252)	0.75 (0.59, 0.81)
Austria	1,949,160	180 (134, 239)	102 (75, 135)	136 (103, 170)	0.76 (0.67, 0.83)
Finland	1,460,602	105 (43, 166)	76 (32, 121)	67 (24, 110)	0.65 (0.47, 0.74)
Croatia	1,101,531	394 (296, 483)	382 (289, 469)	268 (210, 319)	0.68 (0.63, 0.74)
Ireland	1,090,316	13 (5, 22)	18 (7, 30)	9 (4, 15)	0.72 (0.70, 0.75)
Lithuania	1,033,748	74 (15, 173)	73 (15, 170)	50 (10, 109)	0.70 (0.37, 0.90)
Denmark	917,663	22 (13, 31)	27 (16, 38)	17 (10, 23)	0.77 (0.72, 0.80)
Slovakia	877,322	62 (36, 103)	94 (56, 155)	51 (32, 77)	0.83 (0.73, 0.91)
Latvia	874,434	73 (16, 156)	83 (18, 178)	49 (13, 94)	0.67 (0.56, 0.92)
Norway	829,551	52 (23, 77)	81 (36, 119)	30 (14, 43)	0.58 (0.48, 0.66)
Cyprus	457,113	49 (36, 61)	146 (106, 182)	29 (22, 35)	0.59 (0.55, 0.63)
Estonia	440,155	24 (9, 41)	58 (22, 98)	16 (6, 27)	0.70 (0.44, 0.86)
Slovenia	308,320	65 (47, 83)	223 (162, 287)	43 (33, 54)	0.66 (0.61, 0.74)
Malta	170,361	36 (25, 47)	256 (184, 337)	30 (22, 37)	0.83 (0.77, 0.89)
Luxembourg	70,074	7 (5, 9)	119 (88, 150)	4 (3, 5)	0.60 (0.48, 0.67)

Table A2: List of climate models and ensemble members used in the attribution analysis.

ACCESS-CM2_r1i1p1f1	CMCC-CM2-SR5_r1i1p1f1	GFDL-CM4_r1i1p1f1	MIROC-ES2L_r1i1p1f2
ACCESS-ESM1-5_r1i1p1f1	CMCC-ESM2_r1i1p1f1	GFDL-ESM4_r1i1p1f1	MIROC6_r1i1p1f1
AWI-CM-1-1-MR_r1i1p1f1	CNRM-CM6-1-HR_r1i1p1f2	GISS-E2-1-G_r1i1p1f2	MPI-ESM1-2-HR_r1i1p1f1
BCC-CSM2-MR_r1i1p1f1	CNRM-ESM2-1_r1i1p1f2	HadGEM3-GC31-MM_ r1i1p1f3	MRI-ESM2-0_r1i1p1f1
CAMS-CSM1-0_r1i1p1f1	E3SM-1-1_r1i1p1f1	IITM-ESM_r1i1p1f1	NESM3_r1i1p1f1
CanESM5_r1i1p1f1	EC-Earth3_r1i1p1f1	INM-CM4-8_r1i1p1f1	NorESM2-MM_r1i1p1f1
CanESM5-CanOE_r1i1p2f1	EC-Earth3-CC_r1i1p1f1	INM-CM5-0_r1i1p1f1	TaiESM1_r1i1p1f1
CAS-ESM2-0_r1i1p1f1	EC-Earth3-Veg_r1i1p1f1	IPSL-CM6A-LR_r1i1p1f1	UKESM1-0-LL_r1i1p1f2
CESM2-WACCM_r1i1p1f1	FGOALS-f3-L_r1i1p1f1	KACE-1-0-G_r1i1p1f1	
CIESM_r1i1p1f1	FIO-ESM-2-0_r1i1p1f1	MCM-UA-1-0_r1i1p1f2	

Authors

Clair Barnes, Centre for Environmental Policy, Imperial College, London, UK
Garyfallos Konstantinoudis, Grantham Institute for Climate Change and the Environment, Imperial College, London, UK
Pierre Masselot, Environment & Health Modelling Lab, London School of Hygiene and Tropical Medicine, London, UK
Malcolm Mistry, Environment & Health Modelling Lab, London School of Hygiene and Tropical Medicine, London, UK
Antonio Gasparrini, Environment & Health Modelling Lab, London School of Hygiene and Tropical Medicine, London, UK
Ana M Vicedo-Cabrera, Institute of Social and Preventive Medicine, Oeschger Center for Climate Change Research, University of Bern, Bern, Switzerland
Emily Theokritoff, Grantham Institute for Climate Change and the Environment, Imperial College, London, UK
Ben Clarke, Centre for Environmental Policy, Imperial College, London, UK
Friederike Otto, Centre for Environmental Policy, Imperial College, London, UK

Review authors

Sjoukje Philip, Royal Netherlands Meteorological Institute (KNMI), De Bilt, The Netherlands
Mariam Zachariah, Centre for Environmental Policy, Imperial College, London, UK

Media enquiries: grantham.media@imperial.ac.uk

Please cite as:

Barnes, C., et al. (2025). Summer heat deaths in 854 European cities more than tripled due to climate change. Grantham Institute report.
DOI: https://doi.org/10.25560/123873